

# Direct Observation of 4f Intrashell Excitation in Luminescent Eu Complexes by Time-Resolved X-ray Absorption Near Edge Spectroscopy

Joseph I. Pacold,<sup>†</sup> David S. Tatum,<sup>‡,§</sup> Gerald T. Seidler,<sup>\*,†</sup> Kenneth N. Raymond,<sup>‡,§</sup> Xiaoyi Zhang,<sup>||</sup> Andrew B. Stickrath,<sup>⊥,#</sup> and Devon R. Mortensen<sup>†</sup>

<sup>†</sup>Department of Physics, University of Washington, Seattle, Washington 98195, United States

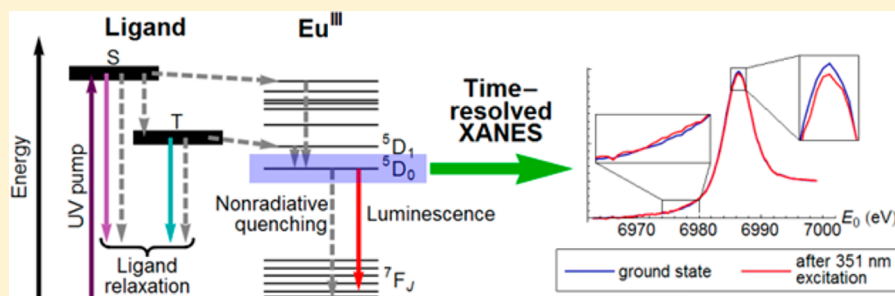
<sup>‡</sup>Chemical Sciences Division, Lawrence Berkeley National Laboratories, Berkeley, California 94720, United States

<sup>§</sup>Department of Chemistry, University of California, Berkeley, California 94720, United States

<sup>||</sup>X-ray Science Division, Argonne National Laboratory, Argonne, Illinois 60439, United States

<sup>⊥</sup>Department of Chemistry, Northwestern University, Evanston, Illinois 60208, United States, and Chemical Sciences and Engineering Division, Argonne National Laboratory, Argonne, Illinois 60439, United States

**S** Supporting Information



**ABSTRACT:** We report time-resolved X-ray absorption near edge structure (TR-XANES) measurements at the Eu  $L_3$  edge upon photoexcitation of several Eu<sup>III</sup>-based luminescent lanthanide complexes. We find an unambiguous signature of the 4f intrashell excitation that occurs upon energy transfer from the photoactive organic antennas to the lanthanide species. Phenomenologically, this observation provides the basis for direct investigation of a crucial step in the energy transfer pathways that lead to sensitized luminescence in lanthanide-based dyes. Interestingly, the details of the TR-XANES feature suggest that the degree of 4f–5d hybridization may itself vary depending on the excited state of the Eu<sup>III</sup> ion.

## INTRODUCTION

Many of the lanthanide elements have useful spectroscopic properties that have spurred broad development of novel luminescent molecules and materials.<sup>1–6</sup> Examples include “standard” phosphors with applications in lighting and communication,<sup>7–10</sup> phosphors with tailored up-conversion or down-conversion properties for the enhancement of photovoltaic cell efficiency,<sup>11–15</sup> and luminescent lanthanide dyes for biological assays,<sup>16–21</sup> in addition to decades of work on laser materials.<sup>22–25</sup> Despite the development of numerous applications, elucidating the energy transfer pathways in luminescent lanthanide materials remains challenging. Most of these systems exploit transitions within the partially filled 4f shells of the trivalent lanthanide ions. The optical cross sections for direct excitation (or de-excitation) of 4f–4f transitions are very weak, since they are electric dipole forbidden by parity and, in some cases, by spin. It is more efficient to indirectly excite the lanthanide by coupling to a sensitizer, i.e., another species that strongly absorbs photons and then transfers energy nonradiatively to the lanthanide.<sup>26–28</sup>

To rationally design efficient luminescent lanthanide materials, it is crucial to understand the underlying mechanisms of energy transfer (which vary from system to system). After initial photoexcitation, the sensitizer may undergo intersystem crossing to lower energy excited states before transferring energy to the lanthanide, creating uncertainty about which particular states contribute most. There are several possible mechanisms for the sensitizer to lanthanide energy transfer, such as resonant Coulomb interactions including Förster dipole–dipole transfer and resonance between higher multipole transitions,<sup>29,30</sup> or charge exchange (Dexter transfer).<sup>31</sup> Resonance conditions and selection rules may constrain these possibilities, but it is often not clear a priori which mechanism is dominant.<sup>32–35</sup> Following energy transfer, the excited state of the lanthanide may relax to a lower excited state before emitting a photon, or be nonradiatively quenched without any photoemission.<sup>36–38</sup>

Received: July 31, 2013

Published: March 7, 2014

Here, we report a time-resolved X-ray absorption near edge spectroscopy (TR-XANES) signature of the ligand-to-lanthanide energy transfer (ET) step in a set of luminescent  $\text{Eu}^{\text{III}}$  complexes. Specifically, we find that photoexcitation of the sensitizing ligand leads to a long-lived ( $> 100 \mu\text{s}$ ) transient change in the XANES at the  $\text{Eu } L_3$  ( $2p_{3/2}$ ) edge, and that the magnitude of the change is correlated with the efficiency of the ligand-to-lanthanide ET. TR-XANES directly interrogates the metal ion and is complementary to time-resolved optical measurements that indirectly provide information about the ET step. While the result we report here is a purely phenomenological observation, we aim to use this ultrafast technique as a time-resolved probe for the excited state electronic structure of  $\text{Eu}^{\text{III}}$  and other lanthanides, toward establishing a more detailed understanding of energy transfer in these systems.

Over the past two decades, TR-XANES has emerged as a powerful technique for studies of transient photoinduced effects, including chemical reactions<sup>39,40</sup> and spin crossover in photoactive transition metal complexes.<sup>41–44</sup> All of these phenomena involve significant distortions in local structure (e.g., dissociation, or bond length changes larger than  $0.1 \text{ \AA}$ ) that are driven by interatomic charge transfer or by electronic occupancy changes in bonding orbitals. Here, we find that TR-XANES can be used to observe a qualitatively different process, the nonradiative transfer of energy to a lanthanide ion, involving no intermediate charge transfer state. Because the long-lived  $\text{Eu}^{\text{III}}$  excitation is confined to nonbonding  $4f$  orbitals, we expect no significant structural change relative to the ground state at the  $100\text{-}\mu\text{s}$  time scale of the observed signal (Supporting Information Figure S4). The nonbonding nature of the  $4f$  orbitals is well documented and self-evident from the atomic-like spectroscopic properties, which is why atomic term symbols are used to label the observed transitions. We note that lanthanide phosphors in general, including those that are sensitized via intermediate charge transfer states, show no difference in configuration coordinate between  $4f$  intrashell excited states.<sup>45–47</sup> It is therefore interesting that we observe a clear TR-XANES feature at all.

The functional form of the transient signal raises questions about the nature of  $4f$  coupling to other atomic orbitals and to the local environment (e.g., the ligand). In particular, we consider whether the degree of  $4f$  mixing with the bonding  $s$ - and  $d$ -orbitals, and consequently the energies of the nominal  $4f$  and  $5d$  manifolds, may itself be a function of  $4f$  excitation.

Luminescent lanthanide dyes<sup>16–21,48–52</sup> such as the ones used in this study provide an illustration of the difficulties involved in understanding the photophysics of a general luminescent lanthanide system. An organic ligand attached to a trivalent lanthanide ion ( $\text{Eu}^{\text{III}}$  here) serves as a light-harvesting antenna<sup>18,26,53</sup> by absorbing broadband UV light (Figure 1). Ideally, this excitation is eventually transferred to the  $\text{Eu}^{\text{III}}$ , which can later emit a visible photon (Figure 1 (a)). The quantum efficiency of this process is limited by the existence of other pathways for radiative and nonradiative dissipation of energy, which we will now summarize. The initial excited singlet state (S) of the ligand may quickly undergo intersystem crossing to the triplet state (T). However, it may also transfer energy directly to the lanthanide, or decay back to the ground state (Figure 1 (c)). When sufficient coupling exists between the ligand and the  $\text{Eu}^{\text{III}}$  ion, a portion of the energy in the ligand S or T state is converted to a  $4f$  intrashell excitation on the  $\text{Eu}^{\text{III}}$ .

The long-lived  $\text{Eu}^{\text{III}}$  excited state requires substantial isolation from solvent species that have vibrational modes capable of quenching the excitation through nonradiative channels<sup>36–38</sup>

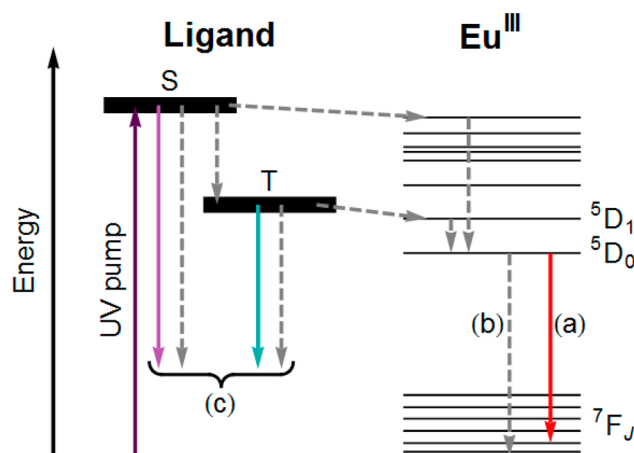


**Figure 1.** A schematic representation of the different possible energy transfer pathways in photoactive luminescent lanthanide complexes. Solid arrows represent radiative transitions, while dashed arrows represent nonradiative transitions. Three possible outcomes of photoexcitation (a, b, c) are described in the text.


(Figure 1 (b)). Ligands used for lanthanide luminescence must therefore be carefully designed to minimize nonradiative solvent coupling. In cases where the excited lanthanide is not quenched, the lanthanide may emit a photon upon  $4f$  intrashell de-excitation along narrow, atomic-like emission lines (Figure 1 (a)). In this final emission step, the intensities of certain  $4f$ – $4f$  transitions, the “hypersensitive” lines (e.g.,  ${}^5\text{D}_0$  to  ${}^7\text{F}_2$  of  $\text{Eu}^{\text{III}}$ ), are strongly dependent on the local environment of the lanthanide atom.<sup>28,54–56</sup>

Each step in this process has been investigated experimentally by UV/visible spectroscopy<sup>28,36,57–59</sup> and by extensive theoretical calculations.<sup>60–64</sup> The overall efficiency of the antenna-to-lanthanide energy transfer has been estimated through calculations based on optical photoemission measurements (as outlined under Materials and Methods) and on the efficiency of energy transfer to a second fluorescent species.<sup>65</sup> Additionally, transient absorption measurements have been used to determine the lifetimes of the various ligand excited states responsible for energy transfer.<sup>58,66</sup> There have been no complementary metal-specific absorption spectroscopy observations of the lanthanide excited state electronic structure, likely due to the very weak, dipole-forbidden nature of the  $4f$  intrashell transitions.

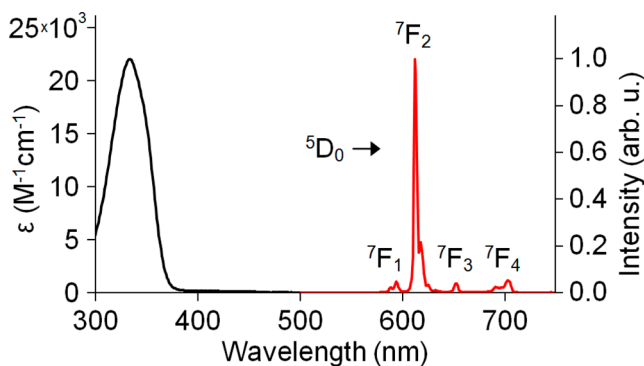
## ■ MATERIALS AND METHODS

The samples are listed in Table 1. The three ligands are similar in that they each bear two 1-hydroxypyridin-2-one amide antennas (Table 1, shown in blue) which bind the  $\text{Eu}^{\text{III}}$  ion through both types of pyridyl oxygen donors. Each ligand has four donors, leading to 8-coordinate 1:2 metal:ligand complexes in the solid state.<sup>48,67</sup> Note that upon solvation, the coordination number of  $[\text{Eu}(\text{L}^2)_2]^-$  increases to nine (Supporting Information Figure S2). The UV–visible absorption and photo-luminescent emission properties of the three complexes are similar. In particular, all three show broadband absorption in the near UV, with the absorption maxima ( $\lambda_{\text{max}}$ ) occurring at wavelengths near 340 nm and similar peak molar absorptivities ( $\epsilon_{\text{max}}$ ). Combined spectra of  $[\text{Eu}(\text{L}^1)_2]^-$  in aqueous buffer are provided in Figure 2 as a representative plot. A notable feature of the luminescence spectrum is the large  ${}^5\text{D}_0 \rightarrow {}^7\text{F}_2$  transition, which accounts for 79% of the total emission.

Analysis of  $\text{Eu}^{\text{III}}$  luminescence is greatly simplified by the presence of a purely magnetic dipole transition ( ${}^5\text{D}_0 \rightarrow {}^7\text{F}_1$ ). With an intensity that is unaffected by the ligand field, the  ${}^5\text{D}_0$  to  ${}^7\text{F}_1$  transition acts as an internal reference for estimating the radiative lifetime ( $\tau_{\text{rad}}$ ). The radiative lifetime, inversely related to the radiative rate ( $k_{\text{rad}}$ ), is the expected  $\text{Eu}^{\text{III}}$

**Table 1. Ligand Structures and Photophysical Parameters of the Luminescent Eu<sup>III</sup> Complexes**


| Complex  | [Eu(L <sup>1</sup> ) <sub>2</sub> ] <sup>-</sup> | [Eu(L <sup>2</sup> ) <sub>2</sub> ] <sup>-</sup> | [Eu(L <sup>3</sup> ) <sub>2</sub> ] <sup>-</sup> |
|--|--|--|--|
| λ <sub>max</sub> (nm)                                | 333  | 337  | 342  |
| ε <sub>max</sub> (M <sup>-1</sup> cm <sup>-1</sup> ) | 22,000   | 19,000   | 21,000   |
| τ <sub>obs</sub> H <sub>2</sub> O (μs)               | 733  | 234  | 536  |
| τ <sub>obs</sub> D <sub>2</sub> O (μs)               | 1022   | 317  | 734  |
| Φ <sub>tot</sub> H <sub>2</sub> O                    | 0.22   | 0.051  | 0.062  |
| τ <sub>rad</sub> (μs)                                | 1680   | 1740   | 1470   |
| k <sub>rad</sub> (s <sup>-1</sup> )                  | 596  | 573  | 680  |
| k <sub>nonrad</sub> (s <sup>-1</sup> )               | 768  | 3700   | 1190   |
| η <sub>Eu</sub>                                      | 0.436  | 0.134  | 0.365  |
| η <sub>sens</sub>                                    | 0.500  | 0.380  | 0.170  |
| q (# of H <sub>2</sub> O)                            | 0.1  | 0.9  | 0.2  |

**Figure 2.** Photoabsorption spectrum (black) and photoluminescence spectrum (red) at 333 nm excitation, collected from a 2 μM solution of [Eu(L<sup>1</sup>)<sub>2</sub>]<sup>-</sup> in 0.1 M Tris buffer (pH = 7.4). Note that the hypersensitive line at 612 nm (<sup>5</sup>D<sub>0</sub> → <sup>7</sup>F<sub>2</sub> transition) dominates the photoemission.

lifetime in the absence of all nonradiative quenching, and it is calculated according to the following equation.<sup>48,56,68</sup>

$$k_{\text{rad}} = 1/\tau_{\text{rad}} = A[I_{\text{tot}}/I_{\text{MD}}] \quad (1)$$

Here,  $I_{\text{tot}}$  and  $I_{\text{MD}}$  are the integrated intensities of the total Eu<sup>III</sup> emission and of the magnetic dipole transition (580 to 600 nm) respectively. The constant,  $A$ , is the spontaneous emission probability of the <sup>5</sup>D<sub>0</sub> to <sup>7</sup>F<sub>1</sub> transition, which is 32.4 s<sup>-1</sup> in water.<sup>68</sup> By comparing the observed luminescent lifetime to the radiative lifetime, we can define the probability that the excited Eu<sup>III</sup> ion will decay radiatively ( $\eta_{\text{Eu}}$ ) as

$$\eta_{\text{Eu}} = \tau_{\text{obs}}/\tau_{\text{rad}} = k_{\text{rad}}/k_{\text{obs}} \quad (2)$$

The overall quantum yields ( $\Phi_{\text{tot}}$ ) were experimentally determined by the optically dilute method using quinine sulfate as the fluorescence standard. The quantum yield is simply the probability that an absorbed UV photon generates an emitted red photon from Eu<sup>III</sup>, and it can be broken down into two component probabilities, the metal efficiency  $\eta_{\text{Eu}}$  defined above and the sensitization efficiency  $\eta_{\text{sens}}$

$$\Phi_{\text{tot}} = (\eta_{\text{sens}})(\eta_{\text{Eu}}) \quad (3)$$

The sensitization efficiency ( $\eta_{\text{sens}}$ ) is the probability that the energy of an absorbed photon is successfully transferred onto the Eu<sup>III</sup> center. The extent of nonradiative quenching of the Eu<sup>III</sup> excited state can be quantified in two ways. First, the rate of nonradiative decay can be calculated using the observed lifetime and calculated radiative lifetime according to the following equation.

$$k_{\text{nonrad}} = k_{\text{obs}} - k_{\text{rad}} = 1/\tau_{\text{obs}} - 1/\tau_{\text{rad}} \quad (4)$$

More specific to aqueous solution, the lifetimes of each complex in H<sub>2</sub>O and D<sub>2</sub>O can be used to determine the degree of Eu<sup>III</sup> hydration. Since O–H oscillators resonate at high energy, water is a particularly efficient quencher of Eu<sup>III</sup> luminescence.<sup>36–38</sup> Consequently, each complex shows a shorter luminescent lifetime in water than deuterated water. The number of inner-sphere water molecules,  $q$ , is calculated using the empirically derived Horrocks equation,<sup>59</sup>

$$q = 1.11(1/\tau_{\text{H}_2\text{O}} - 1/\tau_{\text{D}_2\text{O}} - 0.31) \quad (5)$$

where  $\tau_{\text{H}_2\text{O}}$  and  $\tau_{\text{D}_2\text{O}}$ , the observed luminescent lifetimes in the two solvents, are in milliseconds. Comparing  $k_{\text{nonrad}}$  and  $q$  in Table 1 shows that water coordination leads to increased rates of nonradiative quenching.

Comparing the values  $\eta_{\text{sens}}$  and  $\eta_{\text{Eu}}$  in Table 1 reveals the rationale for choosing these three complexes to study. Complex [Eu(L<sup>1</sup>)<sub>2</sub>]<sup>-</sup> is approximately four times brighter than [Eu(L<sup>2</sup>)<sub>2</sub>]<sup>-</sup> and [Eu(L<sup>3</sup>)<sub>2</sub>]<sup>-</sup> due to efficient sensitization (large  $\eta_{\text{sens}}$ ) and minimal quenching (large  $\eta_{\text{Eu}}$ ;  $q$  close to zero; small  $k_{\text{nonrad}}$ ). Complex [Eu(L<sup>2</sup>)<sub>2</sub>]<sup>-</sup> has efficient sensitization (large  $\eta_{\text{sens}}$ ), but a low quantum yield due to quenching by a bound water molecule (small  $\eta_{\text{Eu}}$ ;  $q$  close to one; large  $k_{\text{nonrad}}$ ). Finally, [Eu(L<sup>3</sup>)<sub>2</sub>]<sup>-</sup> has minimal quenching (large  $\eta_{\text{Eu}}$ ;  $q$  close to zero; small  $k_{\text{nonrad}}$ ) but also a low quantum yield due to inefficient sensitization of the metal (low  $\eta_{\text{sens}}$ ). Thus, complex [Eu(L<sup>1</sup>)<sub>2</sub>]<sup>-</sup> is representative of pathway (a) in Figure 1, [Eu(L<sup>2</sup>)<sub>2</sub>]<sup>-</sup> is representative of (b), and [Eu(L<sup>3</sup>)<sub>2</sub>]<sup>-</sup> is representative of (c). Synthesis and characterization of [Eu(L<sup>2</sup>)<sub>2</sub>]<sup>-</sup> and [Eu(L<sup>3</sup>)<sub>2</sub>]<sup>-</sup> have been reported previously (including further details on the photophysical measurements summarized in Table 1), while [Eu(L<sup>1</sup>)<sub>2</sub>]<sup>-</sup> will be reported soon.<sup>48,67,69</sup>

Time-resolved Eu L<sub>3</sub>-edge XANES measurements were performed in total fluorescence mode at beamline 11-ID-D of the Advanced Photon Source (APS) using a flowing jet of each sample in solution, at concentrations varying from 0.3 to 1 mM. The energy of the incident X-ray beam was scanned through the Eu L<sub>3</sub> edge (i.e., the 2p<sub>3/2</sub> binding energy) in 0.25 eV steps, and the total X-ray fluorescence (proportional to the absorption for a dilute sample) was measured at each step. Avalanche photodiodes were used to record the time-resolved incident X-ray flux and the fluorescence from the sample. A pulsed 351 nm laser was used to excite the chromophore. Data were collected for 300 μs before and after each laser pulse. This collection time was limited by the height of the laser-illuminated volume of sample (approximately 750 μm) and the minimum jet flow rate needed to sustain laminar flow (approximately 3 m/s), rather than the luminescence lifetimes of the samples (τ<sub>obs</sub> H<sub>2</sub>O, Table 1). Additional experimental details are given in the Supporting Information.

## RESULTS AND DISCUSSION

Typical L<sub>3</sub> XANES spectra for [Eu(L<sup>1</sup>)<sub>2</sub>]<sup>-</sup> are shown in Figure 3a. The “white line” peak at 6987 eV corresponds to the 2p<sub>3/2</sub> → 5d excitations dominating the spectrum, since the 5d shell is unoccupied. The width of the peak is determined largely by the splitting of the 5d levels. There is an additional intrinsic broadening of the entire spectrum due to the lifetime of the 2p<sub>3/2</sub> core hole; the implications of this effect are discussed below.

The UV photoexcitation caused a suppression of the white line and additional smaller changes, which are visible in the difference spectra shown in Figure 3b. The difference scales with the pump laser power, saturating (but not changing functional form) near a fluence per shot of 20 mJ/cm<sup>2</sup>; the spectra in Figure 3a were



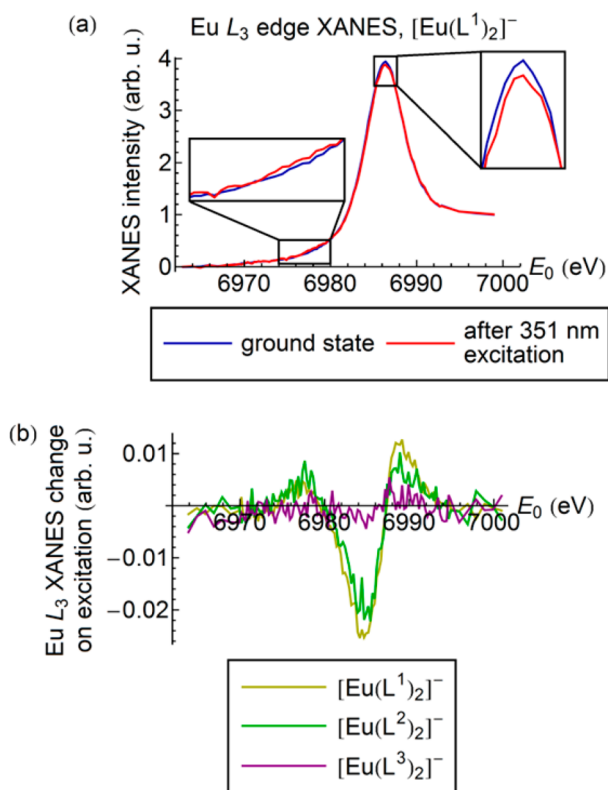


**Figure 3.** (a) Eu  $L_3$  edge XANES collected from a 1 mM solution of  $[\text{Eu}(\text{L}^1)_2]^-$ . The sample was excited by a 351 nm laser with a fluence per pulse of approximately  $20 \text{ mJ}/\text{cm}^2$ . Two sections of the spectrum are magnified (insets) to show part of the change induced by the UV pump. (b) Fractional differences in the excited-state and ground-state XANES from the three complexes used in this study. To mitigate sample damage, the laser fluence was decreased to approximately  $12 \text{ mJ}/\text{cm}^2$  while collecting these spectra, giving a smaller change than the one seen in (a). Data were averaged over  $75 \mu\text{s}$  after the pump pulse to generate the excited-state spectra.

collected at this fluence. The data shown in Figure 3b were collected at a fluence per shot of  $12 \text{ mJ}/\text{cm}^2$ .

The UV pump laser gradually caused sample damage, observed as precipitation of unidentified Eu-containing material out of each solution. Monitoring the intensity of the total fluorescence over time showed that during a typical ten-minute long XANES scan the concentration of Eu in solution decreased by approximately 0.05% (an amount we regard as negligible). The total white line intensity changed by approximately 1% following each laser pulse (Figure 3b). In addition, we observed visible luminescence extending approximately 2 mm along the sample jet below the laser spot. On the basis of the jet flow rate (approximately 3 m/s), we estimate the luminescence lifetime to be on the order of 0.5 ms, consistent with optical measurements.

We first note that the signals from  $[\text{Eu}(\text{L}^1)_2]^-$  and  $[\text{Eu}(\text{L}^2)_2]^-$  have similar magnitudes and shapes, while the signal from  $[\text{Eu}(\text{L}^3)_2]^-$  is strongly suppressed. We find this to be consistent with the calculated  $\eta_{\text{sens}}$  values discussed above; specifically, there is a clear correlation between the magnitude of the transient XANES signal and the efficiency of energy transfer from the ligand to the  $\text{Eu}^{\text{III}}$  ion. The long lifetime ( $>100 \mu\text{s}$ ) of the TR-XANES signal is also inconsistent with the short lifetimes of the ligand excited states of related systems at room temperature ( $<2 \text{ ns}$ ).<sup>58,66</sup> We conclude that the transient signal is a feature of the  $\text{Eu}^{\text{III}}$  4f-4f intrashell excitation that follows photoexcitation of the

antenna, and that X-ray absorption spectroscopy is a useful probe of the transient 4f electronic state of the lanthanide atom in these systems.

Furthermore, we again emphasize that this method specifically targets the lanthanide, and it is therefore complementary to transient absorption and time-resolved photoemission measurements. As a possible application, we suggest that measurements at higher time resolution (available at XFEL facilities) should be able to determine the time delay between UV activation of the ligand and population of the lanthanide 4f excited state(s). This would directly probe the ligand-to-lanthanide energy transfer mechanism in complexes of this type.<sup>32–35,57,70</sup>

Before concluding, it is interesting to consider possible mechanisms for the sensitivity of the  $L_3$  XANES to the 4f intrashell configuration. Recall that this effect is unexpected in light of the insignificant structural differences between the ground state and the excited states of each complex (Supporting Information Figure S3). We therefore consider mechanisms driven purely by changes in electronic structure.

Figure 4a shows a simplified schematic of the density of states of  $\text{Eu}^{\text{III}}$  in the presence of a ligand. The ion has several narrow, atomic-like unoccupied 4f states near the Fermi level  $E_F$ , and a large unfilled 5d band. For clarity, we have plotted a small number of arbitrarily positioned 4f states rather than attempting to show the entire 4f manifold. A simple broadening of the 5d band (Figure 4b) would lead to suppression of the associated XANES peak. This might be caused, for example, by an increase in the crystal field splitting due to a change in the symmetry of the chelating cage around the  $\text{Eu}^{\text{III}}$  ion. However, no such distortion is expected here (Supporting Information Figure S3). As an alternative explanation of our result, we first note that there is a TR-XANES peak at 6977 eV. We expect unoccupied 4f states (or mixed 4f–5d states) to contribute to the XANES near this energy, since FEFF calculations<sup>71</sup> (Supporting Information Figure S8) show a concentration of Eu f states there. In addition, this energy is 10 eV below the white-line peak, and the gap between the 4f and 5d levels of  $\text{Eu}^{\text{III}}$  is on the order of 10 eV in solid-state systems.<sup>72–74</sup>

Taken together, the TR-XANES features of the long-lived  $\text{Eu}^{\text{III}}$  excited state indicate a change in both the 4f and 5d states, as would be associated with an increase of 4f–5d mixing (Figure 4c). As support for this hypothesis, we note that *static* orbital hybridization effects in lanthanide materials have been extensively studied.<sup>75–77</sup> In particular, quantitative interpretations of visible lanthanide emission spectra<sup>78–81</sup> use 4f wave functions that are mixed with opposite-parity 5d states due to perturbation by the ligand field. The observation of a *time-dependent* change in the degree of orbital mixing would have important consequences for theoretical calculations of the energy transfer rate, as well as for treatments of the emission spectrum in these complexes.

The total fluorescence detection method used in this experiment gives spectra with an energy resolution intrinsically limited by the 3.91 eV lifetime of the  $2p_{3/2}$  vacancy. The low resolution destroys some information about the density of states, especially changes of the hypothetical type shown in Figure 4. The present data therefore do not distinguish unambiguously between the possible scenarios. Existing data on lanthanide compounds,<sup>82–85</sup> including europium(III) oxide,<sup>74</sup> show that it is possible to resolve 2p to 4f excitations with high detection energy resolution; further studies are ongoing.

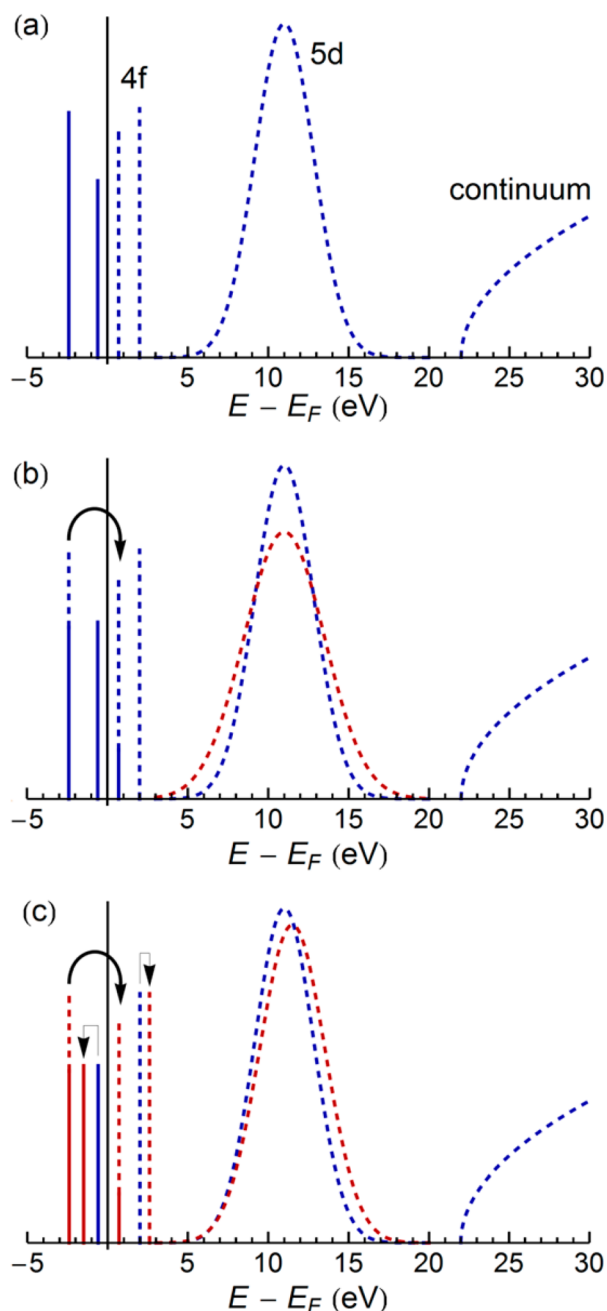


**Figure 4.** (a) Schematic representation of the density of states for ground-state  $\text{Eu}^{\text{III}}$ , including atomic-like occupied 4f states (solid lines), unoccupied 4f states (dashed), and unoccupied 5d and continuum bands. (b) Effect of a 4f–4f transition accompanied by a change in 5d crystal field splitting. (c) Effect of a 4f–4f excitation accompanied by a change in the degree of 4f–5d hybridization. The curved arrows indicate the change in electron occupancy upon excitation, while the orthogonal arrows indicate reorganization of the 4f manifold due to a changed 4f–5d hybridization.

## SUMMARY

We have identified a transient XANES signal associated with the 4f–4f intrashell transition that precedes hypersensitive emission in a family of luminescent Eu complexes. The functional form of the transient signal suggests that excitation-induced orbital hybridization effects may play an unexpected role in systems of the type studied here. More fundamentally, the existence of the signal demonstrates that time-resolved X-ray absorption spec-

troscopy is a promising tool for directly studying the excited states of lanthanides in luminescent materials.

## ASSOCIATED CONTENT

### Supporting Information

DFT-minimized structures of the ground states; structure comparison of the S and T state for  $[\text{Eu}(\text{L})_2]^-$ ; additional details on collection of TR-XANES; analysis of laser-induced and X-ray-induced sample damage; results of FEFF calculations of the *l*-projected density of states. This material is available free of charge via the Internet at <http://pubs.acs.org>.

## AUTHOR INFORMATION

### Corresponding Author

seidler@uw.edu

### Present Address

#A.B.S.: Booz Allen Hamilton, Inc., Arlington, Virginia 22203, United States.

### Notes

The authors declare no competing financial interest.

## ACKNOWLEDGMENTS

G.T.S. and K.N.R. acknowledge support of this research program by the U.S. Department of Energy, Basic Energy Sciences, by Grant No. DE-FG02-09ER16106 and Contract No. DE-AC02-05CH11231, respectively. D.R.M. was in part supported by the Chemical Imaging Initiative at Pacific Northwest National Laboratory, under the Laboratory Directed Research and Development Program at PNNL, a multiprogram national laboratory operated by Battelle for the U.S. Department of Energy. Laser facilities at 11-ID-D were provided by the Solar Energy Conversion group of the Chemical Sciences and Engineering Division of Argonne National Laboratory, which is funded through New Facility and Midscale Instrumentation grants to Lin X. Chen et al. Use of the Advanced Photon Source, an Office of Science User Facility operated for DOE Office of Science by Argonne National Laboratory, was supported by the U.S. DOE under Contract No. DE-AC02-06CH11357.

## REFERENCES

- Eliseeva, S. V.; Bunzli, J. C. G. *New J. Chem.* **2011**, *35*, 1165.
- Bunzli, J. C. G.; Eliseeva, S. V. *J. Rare Earth* **2010**, *28*, 824.
- Bunzli, J. C. G.; Piguet, C. *Chem. Soc. Rev.* **2005**, *34*, 1048.
- Binnemans, K. *Chem. Rev.* **2009**, *109*, 4283.
- de Sa, G. F.; Malta, O. L.; Donega, C. D.; Simas, A. M.; Longo, R. L.; Santa-Cruz, P. A.; da Silva, E. F. *Coord. Chem. Rev.* **2000**, *196*, 165.
- Eliseeva, S. V.; Bunzli, J. C. G. *Chem. Soc. Rev.* **2009**, *39*, 189.
- Ronda, C. R.; Justel, T.; Nikol, H. *J. Alloys Compd.* **1998**, *275*, 669.
- Shur, M. S.; Zukauskas, A. *Proc. IEEE* **2005**, *93*, 1691.
- Kim, J. S.; Jeon, P. E.; Park, Y. H.; Choi, J. C.; Park, H. L.; Kim, G. C.; Kim, T. W. *Appl. Phys. Lett.* **2004**, *85*, 3696.
- Miniscalco, W. J. *J. Lightwave Technol.* **1991**, *9*, 234.
- Wegh, R. T.; Donker, H.; Oskam, K. D.; Meijerink, A. *Science* **1999**, *283*, 663.
- Trupke, T.; Shalav, A.; Richards, B. S.; Wurfel, P.; Green, M. A. *Sol. Energy Mater. Sol. Cells* **2006**, *90*, 3327.
- Richards, B. S. *Sol. Energy Mater. Sol. Cells* **2006**, *90*, 2329.
- Richards, B. S. *Sol. Energy Mater. Sol. Cells* **2006**, *90*, 1189.
- van der Ende, B. M.; Aarts, L.; Meijerink, A. *Phys. Chem. Chem. Phys.* **2009**, *11*, 11081.
- Soini, E.; Lovgren, T. *Crit. Rev. Anal. Chem.* **1987**, *18*, 105.
- Handl, H. L.; Gillies, R. J. *Life Sci.* **2005**, *77*, 361.
- Petoud, S.; Cohen, S. M.; Bunzli, J. C. G.; Raymond, K. N. *J. Am. Chem. Soc.* **2003**, *125*, 13324.

- (19) Parker, D.; Williams, J. A. G. *J. Chem. Soc., Dalton Trans.* **1996**, 3613.
- (20) Moore, E. G.; Samuel, A. P. S.; Raymond, K. N. *Acc. Chem. Res.* **2009**, *42*, 542.
- (21) Selvin, P. R. *Annu. Rev. Biophys. Biomol. Struct.* **2002**, *31*, 275.
- (22) Reisfeld, R.; Jørgensen, C. K. I. *Lasers and Excited States of Rare Earths*; Springer-Verlag: Berlin ; New York, 1977.
- (23) Kuriki, K.; Koike, Y.; Okamoto, Y. *Chem. Rev.* **2002**, *102*, 2347.
- (24) Weber, J. K. R.; Felten, J. J.; Cho, B.; Nordine, P. C. *Nature* **1998**, *393*, 769.
- (25) Slooff, L. H.; van Blaaderen, A.; Polman, A.; Hebbink, G. A.; Klink, S. I.; Van Veggel, F. C. J. M.; Reinhoudt, D. N.; Hofstraat, J. W. J. *Appl. Phys.* **2002**, *91*, 3955.
- (26) Weissman, S. I. *J. Chem. Phys.* **1942**, *10*, 214.
- (27) Nakazawa, E. In *Fundamentals of Phosphors*; Yen, W. M. Shionoya, S.; Yamamoto, H., Ed.; CRC Press: Boca Raton, FL, 2006; p 89.
- (28) Bunzli, J. C. G. Eliseeva, S. V. In *Lanthanide Luminescence*; Aspinall, H. C., Ed.; Springer: Berlin, Heidelberg, 2011; p 1.
- (29) Forster, T. *Discuss. Faraday Soc.* **1959**, 7.
- (30) Forster, T. *Chem. Phys. Lett.* **1971**, *12*, 422.
- (31) Dexter, D. L. *J. Chem. Phys.* **1953**, *21*, 836.
- (32) Lima, P. P.; Nobre, S. S.; Freire, R. O.; Junior, S. A.; Ferreira, R. A. S.; Pischel, U.; Malta, O. L.; Carlos, L. D. *J. Phys. Chem. C* **2007**, *111*, 17627.
- (33) Ward, M. D. *Coord. Chem. Rev.* **2010**, *254*, 2634.
- (34) Hebbink, G. A.; Klink, S. I.; Grave, L.; Alink, P. G. B. O.; van Veggel, F. C. J. M. *ChemPhysChem* **2002**, *3*, 1014.
- (35) Hebbink, G. A.; Grave, L.; Woldering, L. A.; Reinhoudt, D. N.; van Veggel, F. C. J. M. *J. Phys. Chem. A* **2003**, *107*, 2483.
- (36) Heller, A. *J. Am. Chem. Soc.* **1966**, *88*, 2058.
- (37) Haas, Y.; Stein, G. *J. Phys. Chem.* **1971**, *75*, 3677.
- (38) Kropp, J. L.; Windsor, M. W. *J. Chem. Phys.* **1965**, *42*, 1599.
- (39) Stickrath, A. B.; Mara, M. W.; Lockard, J. V.; Harpham, M. R.; Huang, J.; Zhang, X. Y.; Attenkofer, K.; Chen, L. X. *J. Phys. Chem. B* **2013**, *117*, 4705.
- (40) Chen, L. X.; Zhang, X. Y.; Lockard, J. V.; Stickrath, A. B.; Attenkofer, K.; Jennings, G.; Liu, D. J. *Acta Crystallogr., Sect. A* **2010**, *66*, 240.
- (41) Bressler, C.; Milne, C.; Pham, V. T.; ElNahhas, A.; van der Veen, R. M.; Gawelda, W.; Johnson, S.; Beaud, P.; Grolimund, D.; Kaiser, M.; Borca, C. N.; Ingold, G.; Abela, R.; Chergui, M. *Science* **2009**, *323*, 489.
- (42) Huse, N.; Kim, T. K.; Jamula, L.; McCusker, J. K.; de Groot, F. M. F.; Schoenlein, R. W. *J. Am. Chem. Soc.* **2010**, *132*, 6809.
- (43) Monat, J. E.; McCusker, J. K. *J. Am. Chem. Soc.* **2000**, *122*, 4092.
- (44) Gawelda, W.; Pham, V. T.; Benfatto, M.; Zaushitsyn, Y.; Kaiser, M.; Grolimund, D.; Johnson, S. L.; Abela, R.; Hauser, A.; Bressler, C.; Chergui, M. *Phys. Rev. Lett.* **2007**, *98*, 057401.
- (45) Blasse, G.; Grabmeier, B. C. *Luminescent Materials*; Springer-Verlag: Berlin, 1994.
- (46) Fonger, W. H.; Struck, C. W. *J. Chem. Phys.* **1970**, *52*, 6364.
- (47) Struck, C. W.; Fonger, W. H. *J. Chem. Phys.* **1976**, *64*, 1784.
- (48) D'Aleo, A.; Moore, E. G.; Szigethy, G.; Xu, J.; Raymond, K. N. *Inorg. Chem.* **2009**, *48*, 9316.
- (49) Moore, E. G.; Xu, J. D.; Jocher, C. J.; Werner, E. J.; Raymond, K. N. *J. Am. Chem. Soc.* **2006**, *128*, 10648.
- (50) Moore, E. G.; Xu, J. D.; Jocher, J.; Castro-Rodriguez, I.; Raymond, K. N. *Inorg. Chem.* **2008**, *47*, 3105.
- (51) Fernandez-Moreira, V.; Song, B.; Sivagnanam, V.; Chauvin, A. S.; Vandevyver, C. D. B.; Gijss, M.; Hemmila, I.; Lehr, H. A.; Bunzli, J. C. G. *Analyst* **2010**, *135*, 42.
- (52) Moore, E. G.; Xu, J. D.; Jocher, C. J.; Corneillie, T. M.; Raymond, K. N. *Inorg. Chem.* **2010**, *49*, 9928.
- (53) Crosby, G. A.; Kasha, M. *Spectrochim. Acta* **1958**, *10*, 377.
- (54) Moeller, T.; Ulrich, W. F. *J. Inorg. Nucl. Chem.* **1956**, *2*, 164.
- (55) Sonesson, A. *Acta Chem. Scand.* **1958**, *12*, 1937.
- (56) Werts, M. H. V.; Jukes, R. T. F.; Verhoeven, J. W. *Phys. Chem. Chem. Phys.* **2002**, *4*, 1542.
- (57) Yang, C.; Fu, L. M.; Wang, Y.; Zhang, J. P.; Wong, W. T.; Ai, X. C.; Qiao, Y. F.; Zou, B. S.; Gui, L. L. *Angew. Chem., Int. Ed.* **2004**, *43*, 5010.
- (58) Moore, E. G.; Grilj, J.; Vauthey, E.; Ceroni, P. *Dalton Trans.* **2013**, *42*, 2075.
- (59) Supkowski, R. M.; Horrocks, W. D. *Inorg. Chim. Acta* **2002**, *340*, 44.
- (60) Malta, O. L. *J. Lumin.* **1997**, *71*, 229.
- (61) Malta, O. L. *J. Non-Cryst. Solids* **2008**, *354*, 4770.
- (62) Rodrigues, M. O.; da Costa, N. B.; de Simone, C. A.; Araujo, A. A. S.; Brito-Silva, A. M.; Paz, F. A. A.; de Mesquita, M. E.; Junior, S. A.; Freire, R. O. *J. Phys. Chem. B* **2008**, *112*, 4204.
- (63) Malta, O. L.; Legendziewicz, J.; Huskowska, E.; Turowska-Tyrk, I.; Albuquerque, R. Q.; Donega, C. D.; Silva, F. R. G. E. *J. Alloys Compd.* **2001**, *323*, 654.
- (64) Malta, O. L.; Batista, H. J.; Carlos, L. D. *Chem. Phys.* **2002**, *282*, 21.
- (65) Xiao, M.; Selvin, P. R. *J. Am. Chem. Soc.* **2001**, *123*, 7067.
- (66) Foley, T. J.; Harrison, B. S.; Knefely, A. S.; Abboud, K. A.; Reynolds, J. R.; Schanze, K. S.; Boncella, J. M. *Inorg. Chem.* **2003**, *42*, 5023.
- (67) D'Aleo, A.; Xu, J.; Moore, E. G.; Jocher, C. J.; Raymond, K. N. *Inorg. Chem.* **2008**, *47*, 6109.
- (68) Beeby, A.; Bushby, L. M.; Maffeo, D.; Williams, J. A. G. *J. Chem. Soc., Dalton Trans.* **2002**, 48.
- (69) Tatum, D. Manuscript in preparation, 2014.
- (70) Rodriguez-Cortinas, R.; Avecilla, F.; Platas-Iglesias, C.; Imbert, D.; Bunzli, J. C. G.; de Blas, A.; Rodriguez-Blas, T. *Inorg. Chem.* **2002**, *41*, 5336.
- (71) Rehr, J. J.; Kas, J. J.; Vila, F. D.; Prange, M. P.; Jorissen, K. *Phys. Chem. Chem. Phys.* **2010**, *12*, 5503.
- (72) Thiel, C. W.; Cone, R. L. *J. Lumin.* **2011**, *131*, 386.
- (73) Dorenbos, P. *J. Lumin.* **2000**, *91*, 91.
- (74) Yamaoka, H.; Taguchi, A.; Vlaicu, A. M.; Oohashi, H.; Yokoi, K.; Horiguchi, D.; Tochio, T.; Ito, Y.; Kawatsura, K.; Yamamoto, K.; Chainani, A.; Shin, S.; Shiga, M.; Wada, H. *J. Phys. Soc. Jpn.* **2006**, *75*, 034702.
- (75) Strange, P.; Svane, A.; Temmerman, W. M.; Szotek, Z.; Winter, H. *Nature* **1999**, *399*, 756.
- (76) Brown, S. D.; Strange, P.; Bouchenoire, L.; Zarychta, B.; Thompson, P. B. J.; Mannix, D.; Stockton, S. J.; Horne, M.; Arola, E.; Ebert, H.; Szotek, Z.; Temmerman, W. M.; Fort, D. *Phys. Rev. Lett.* **2007**, *99*, No. 247401.
- (77) Brown, S. D.; Strange, P.; Bouchenoire, L.; Thompson, P. B. J. *Phys. Rev. B* **2013**, *87*, No. 165111.
- (78) Judd, B. R. *J. Chem. Phys.* **1966**, *44*, 839.
- (79) Judd, B. R. *J. Chem. Phys.* **1979**, *70*, 4830.
- (80) Ofelt, G. S. *J. Chem. Phys.* **1962**, *37*, 511.
- (81) Mason, S. F.; Peacock, R. D.; Stewart, B. *Mol. Phys.* **1975**, *30*, 1829.
- (82) Krisch, M. H.; Kao, C. C.; Sette, F.; Caliebe, W. A.; Hamalainen, K.; Hastings, J. B. *Phys. Rev. Lett.* **1995**, *74*, 4931.
- (83) Bartolome, F.; Krisch, M. H.; Raoux, D.; Tonnerre, J. M. *Phys. Rev. B* **1999**, *60*, 13497.
- (84) Dallera, C.; Krisch, M. H.; Rogalev, A.; Gauthier, C.; Goulon, J.; Sette, F.; Sole, A. *Phys. Rev. B* **2000**, *62*, 7093.
- (85) Hamalainen, K.; Siddons, D. P.; Hastings, J. B.; Berman, L. E. *Phys. Rev. Lett.* **1991**, *67*, 2850.